PHYSICAL REVIEW C **74**, 042201(R) (2006)

Charged- and neutral-pion production in the *S*-matrix approach

V. Malafaia,[1] M. T. Peña,[1,2] Ch. Elster,[3] and J. Adam, Jr.[4]
[1]*Centro de Física Teórica de Partículas, Instituto Superior Técnico*
[2]*Department of Physics, Instituto Superior Técnico, Av. Rovisco Pais, P-1049-001 Lisbon, Portugal*
[3]*Institute of Nuclear and Particle Physics, and Department of Physics and Astronomy, Ohio University, Athens, Ohio 45701, USA*
[4]*Nuclear Physics Institute, Řež CZ-25068, Czech Republic*
(Received 15 November 2005; published 31 October 2006)

The *S*-matrix approach is used to calculate both charged- and neutral-pion production in nucleon-nucleon (*NN*) scattering near threshold. The irreducible pion-rescattering diagram, direct production mechanism, Δ isobars in intermediate states, and Z diagrams mediated by heavy isoscalar mesons are included in the calculation. For the *NN* distortions, we considered a realistic interaction, within the Bonn family of potentials, which describes the nucleonic inelasticities above the pion production energy threshold.

DOI: 10.1103/PhysRevC.74.042201 PACS number(s): 13.60.Le, 21.45.+v, 25.10.+s, 25.40.Ve

The description of pion production from two-nucleon collisions very near threshold is a difficult and interesting problem, which still presents open issues as documented in recent reviews [1] and calculations [2]. At threshold, chiral symmetry suppresses the direct production from one nucleon, and the production cross section results from a delicate balance of various contributions. A further challenge is posed by the interaction between the colliding nucleons, which is not as well known above the pion production threshold as it is below.

The reactions considered here are characterized by above-threshold energies of the incoming nucleons, a relatively large momentum- and energy-transfer in the pion emission, and the suppression of direct production from a single nucleon. In the model-independent framework of chiral perturbation theory (χPT) this requires the modification of the counting scheme and a careful evaluation of contributions beyond leading order [2,3] such as chiral loops. Most of these chiral loops were calculated right at threshold kinematics. The effective operators derived from the χPT should in principle be used with a χPT *NN* interaction, which is not yet established above the pion threshold. When one moves very far from the threshold, both the transition operators and the *NN* interactions have to be constructed in dynamic coupled channel approaches (see, e.g., Ref. [4]).

Our calculations do not compete with these elaborate approaches; we claim that close to the threshold it might be sufficient to use a simplified model based on a one-meson-exchange picture and the *S*-matrix prescription described next. We focus on the energy dependence of the production operators obtained in this way, and we also adopt a realistic *NN* interaction, valid below and well above the production threshold. Our calculation of the cross sections for all isospin channels near threshold includes a sufficient number of final state three-body basis states and employs a newly developed *NN* interaction tuned at energies above the pion production threshold. In these aspects, our results are to be viewed as complementary to those more fundamental approaches mentioned above.

Various model calculations indicated that apart from two-nucleon operators of the pion range, those mediated by effective σ and ω meson exchange should also be considered [1,5]. As for the Δ-isobar resonance, it plays a role since the excitation energy of this resonance is close to the energy exchange demanded by pion production [6], but at threshold, chiral symmetry makes relevant the full content of the πN scattering amplitude.

Therefore, we include here (i) the usual direct single-nucleon production operator, (ii) the pion-rescattering diagram (see Refs. [7–10]) which contains the πN scattering amplitude, and (iii) the Z diagrams mediated by exchanges of a single σ or ω meson [5] to represent short-range effects. In Ref. [7], it is explained why this approach is a good approximation for calculations with phenomenological *NN* interactions. In particular, the effective σ or ω exchange Z diagrams represent the chiral short-range contact terms and, as mentioned in Ref. [8], some multipion-exchange diagrams.

We start with transition amplitudes for pion production defined as matrix elements of an effective pion production nuclear operator between initial and final state *NN* wave functions. We represent the operators of the model irreducible reaction mechanisms by Feynman diagrams, with free uncorrelated on-mass-shell nucleons before and after pion emission. The total energy is conserved, i.e., these diagrams define the corresponding operators on-energy shell. However, when sandwiched between correlated nucleon wave functions, the integration over the intermediate momenta necessarily brings these operators off-energy-shell. Thus an uncertainty arises about how to treat the energy transfer occurring in the effective operators, e.g., how to define the energy and retardation of the exchanged mesons. Two methods appeared in the literature dealing with this problem for pion production operators, in particular for the pion rescattering one. First, the energy of the exchanged pion was fixed by some prescriptions [5,7,8,11,12] so that the matrix elements can easily be calculated. Although such simple prescriptions facilitate similar calculations for heavier nuclei, the $pp \to pp\pi^0$ cross section was shown to be rather sensitive to them [11–13]. Second, more recently [11], for diagrams with pion rescattering distorted by single-meson exchange in the initial or final state, the energy dependence of the production operator was derived by reducing these diagrams from a covariant to a time-ordered form. In Refs. [11,14] it was demonstrated that the latter procedure

defines different operators from the initial state interaction (ISI) and final state interaction (FSI) diagrams for pion rescattering. We have shown [13] that these two operators can be very well approximated by a simple S-matrix prescription for the energy of the exchanged pion in the $pp \to pp\pi^0$ reaction near threshold. In this work, we also adopt this S-matrix approach for the other pion production reactions.

For the pion-rescattering diagram (Fig. 1), the S-matrix prescription yields in a shorthand notation [13]

$$\hat{O}^S_{rs} = \frac{f(\Omega)}{(\Omega)^2 - \left(m_\pi^2 + \vec{q}\,'^2\right)}, \tag{1}$$

$$\Omega = \frac{(E_2 - \omega_2)}{2} + \frac{(\omega_1 + E_\pi - E_1)}{2}, \tag{2}$$

where, as in Ref. [14], E_1, E_2, ω_1, and ω_2 are the nucleon on-shell energies before and after pion emission. $E_\pi\,(\vec{q}_\pi)$ is the energy (three-momentum) of the emitted pion, $\Omega\,(\vec{q}\,')$ is the exchanged pion energy (three-momentum), and $f(\Omega)$ is the product of the πN amplitude with the πNN vertex. Its isospin-nonflip part is derived from [10] and reads

$$f_{\rm nonflip}(\Omega) = i\frac{g_A}{f_\pi^3}\left\{\left[2c_1 m_\pi^2 - \left(c_2 + c_3 - \frac{g_A^2}{8M}\right)\Omega E_\pi + c_3 \vec{q}_\pi \cdot \vec{q}\,'\right]\tau_a^{(2)} + \frac{\delta_q}{8}\left[\tau_a^{(1)}\tau_3^{(2)} + \delta_{3a}(\tau^{(1)}\cdot\tau^{(2)})\right]\right\}\vec{\sigma}^{(2)}\cdot\vec{q}\,', \tag{3}$$

where δ_q is the quark mass difference contribution to the neutron-proton mass splitting. For the low-energy constants, we took the values $c_1 = -0.93$, $c_2 = 3.34$, and $c_3 = -5.29$ according to Ref. [15]. We tested also another set of values adopted in Ref. [16], but the results near threshold were not very sensitive to those parameter changes. For the isospin-flip part, the isovector Weinberg-Tomozawa term with Galilean corrections [10] is employed to obtain

$$f_{\rm flip}(\Omega) = -\frac{g_A}{8f_\pi^3}\epsilon_{abc}\tau_b^{(1)}\tau_c^{(2)} \times \left[(\Omega + E_\pi) - \frac{1}{2M} \times (\vec{p} + \vec{p}\,' - \vec{q}_\pi/2)\cdot(\vec{q}_\pi + \vec{q}\,')\right]\vec{\sigma}^{(2)}\cdot\vec{q}\,', \tag{4}$$

where a, b, and c are isospin indices, in particular, a labels the emitted pion; and ϵ_{abc} is the Levi-Civita tensor. The initial (final) two-nucleon relative momentum is $\vec{p}\,(\vec{p}\,')$. The constants g_A and f_π are the axial-vector coupling of the nucleon and the pion decay constant, respectively.

The symmetric implementation of Eq. (2) for the energy conservation at the two vertices of the diagram of Fig. 1 is used. This prescription minimizes the deviation between the S matrix and the time-ordered perturbation theory (TOPT) results for the rescattering isoscalar diagram [13]. Here the S-matrix approach is used for all the two-nucleon mechanisms considered. Other prescriptions have been suggested in the literature: the static approximation ($\Omega \to 0$), the fixed kinematics approximation ($\Omega \to m_\pi/2$), and the E-E' approximation, here called on-shell approximation ($\Omega \to E_2 - \omega_2$). They were shown to deviate considerably from the TOPT

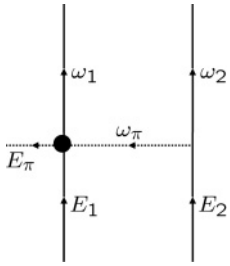

FIG. 1. The re-scattering diagram and definitions of variables for the on-mass-shell energies of the different legs.

results for the $pp \to pp\pi^0$ cross section [13]. Here we also test them in the charged-pion channels.

The explicit Δ-isobar propagation contribution is given by

$$f_\Delta(\Omega) = i\frac{h_A^2 g_A}{72 f_\pi^3}\vec{\sigma}^{(2)}\cdot\vec{q}\,'\left\{\left[2\tau_a^{(2)} - i\epsilon_{abc}\tau_b^{(2)}\tau_c^{(1)}\right]\left[2\vec{q}_\pi\cdot\vec{q}\,' + i\vec{\sigma}^{(1)}\cdot(\vec{q}\,'\times\vec{q}_\pi)\right]G_\Delta^{(I)} + \left[2\tau_a^{(2)} + i\epsilon_{abc}\tau_b^{(2)}\tau_c^{(1)}\right] \times \left[2\vec{q}_\pi\cdot\vec{q}\,' - i\vec{\sigma}^{(1)}\cdot(\vec{q}\,'\times\vec{q}_\pi)\right]G_\Delta^{(II)}\right\}, \tag{5}$$

where h_A is the $\Delta\pi N$ coupling. The Δ propagators are given by $G_\Delta^{(I)} = (E_\pi + F_1 - m_\Delta)^{-1}$ and $G_\Delta^{(II)} = (E_1 - E_\pi - m_\Delta)^{-1}$, with E_1 and F_1 being the initial and final nucleon energy, respectively.

In its term proportional to c_3, the πN rescattering amplitude includes part of the effects of the Δ given by Eq. (5). Therefore, when the pion rescattering through a virtual Δ isobar is included explicitly by means of Eq. (5), its static limit, when $F_1 \to M$, $E_1 \to M + m_\pi/2$, and $E_\pi \to m_\pi$, is subtracted from the πN scattering amplitude Eq. (3), to avoid double counting. This redefines the parameter $c_3 = -5.29$ GeV^{-1} to $c_3' = c_3 - \tilde{c_3}^\Delta$, with $\tilde{c_3}^\Delta = -3.66$ GeV^{-1}. We checked that the results obtained using the full πN scattering amplitude of Eq. (3) do not differ much from those obtained when the Δ propagation is added, as in Eq. (5), provided the replacement $c_3 \to \tilde{c}_3^\Delta$ is done. The direct production term and the σ and ω Z diagrams are taken as in Ref. [5]. All αNN (where $\alpha = \pi, \sigma, \omega$) and $\pi N\Delta$ vertices are multiplied by the same hadronic form factors as used in the NN potential. The masses and coupling constants are also taken from the NN interaction used for the initial and final nucleonic states.

For the initial state, the nucleon-nucleon interaction is necessarily needed above the pion production threshold, where phase-shift analysis provides the nonvanishing inelasticity parameter ρ, indicating the onset of inelastic channels in the NN interaction. An obvious way to include these channels into the NN interaction is through nucleon resonances, which predominantly decay into a nucleon and a pion, as the P_{33} (Δ) and the P_{11} ($N^*(1440)$). This is how the recently developed model of the Ohio group, based on [17], is constructed to describe the NN scattering data [18]. It contains the two resonances mentioned as intermediate states in two-meson-exchange iterative diagrams. The two resonances are described by a Breit-Wigner type function, fitted to the experimental widths. The model parameters are given in Table I. Details will follow in Ref. [19]. We compare cross sections calculated with the Ohio and the Bonn-B potentials [20], the last

TABLE I. Parameters for vertices of the Ohio NN interaction. The meson mass is m_α, the coupling constants are g and f, and Λ is the cutoff parameter at the vertex.

Vertex	Meson	m_α [MeV]	$\frac{g^2_{NN\alpha}}{4\pi}$	f_α/g_α	$\Lambda_{NN\alpha}$ [MeV]
$NN\alpha$	π	138.03	13.8		1498
	η	547.3	2.00		1300
	ω	782.6	23.6		1396
	ρ	769	1.1	5.9	1281
	a_0	980	4.75		1004
	$\sigma(T=1)$	494	5.26		1924
	$\sigma(T=0)$	495	3.593		1700
	η'	958	1.62		1433
	f_0	980	2.50		1471
			$\frac{f^2_{N\Delta\alpha}}{4\pi}$		$\Lambda_{N\Delta\alpha}$ [MeV]
$N\Delta\alpha$	π	138.03	0.224		677
	ρ	769	20.45		1508
$NN^*(1440)\alpha$	π	138.03	0.035		800
	σ	494	0.015		1119

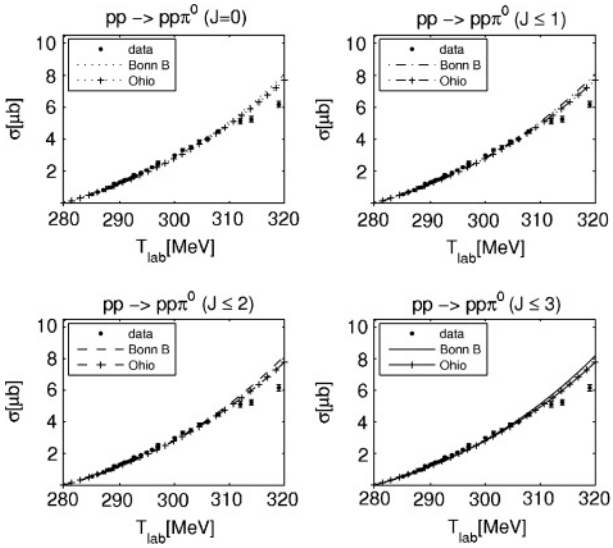

FIG. 3. $pp \to pp\pi^0$ cross section. Dotted ($J=0$), dashed-dotted ($J \leqslant 1$), dashed ($J \leqslant 2$), and solid ($J \leqslant 3$) lines with (without) +'s correspond to the Ohio (Bonn B) potential. Data points are from Ref. [21].

one representing a generic one-boson-exchange model valid below the pion production threshold. The explicit inclusion of iterative diagrams introduces an energy dependence into the potential, despite the meson propagators themselves being energy independent.

In Fig. 2, we compare the cross sections calculated within the S-matrix approach against those obtained with the frequently used (static, fixed kinematics, and on-shell) approximations discussed above. For all charge channels, the deviation is largest for the static approximation, which overestimates the cross sections by a factor larger than 2 (close to threshold). The E-E' (on-shell) approximation also deviates from the reference S-matrix result. At threshold, it may be off at maximum by 20% for all cases. For π^0 production, the fixed kinematics approximation practically coincides with the S matrix, with the largest deviations at high energies. The deviation from unity in the cross section ratios of Fig. 2 is mainly due to the energy dependence of the rescattering term. Moreover, as found in Ref. [13], the dominant energy dependence of that term comes from the rescattering vertex, with the sensitivity to the energy prescription in the pion propagator being much smaller. For the heavier mesons in the Z diagrams, the sensitivity to the energy in the propagators is further suppressed by the larger masses involved, making the pion rescattering decisive for the results of the ratios. In Figs. 3–5 we compare the cross sections calculated with the Ohio and the Bonn-B interactions and simultaneously illustrate the convergence of the amplitude partial waves with increasing total angular momentum J. In both potentials, the meson propagators are static. However, in contrast to Bonn-B, the Ohio potential carries energy dependence in the propagators of the iterative diagrams with the $N\Delta$ and NN^* intermediate states. This energy dependence is compatible with the energy prescription used for the pion production operator, since both particles are on-mass shell in intermediate states, consistent with the S-matrix prescription of Eq. (2). We note that perfect consistency would call for retardation in the meson propagators of the potential as well as in the re-scattering production operator. However, the energy prescription in the vertex (and consequently the energy for the intermediate N^* in the boxes) dominates over the retardation effects in the meson propagators as shown in Ref. [13], justifying the use of potentials which use static meson propagators.

Very close to threshold, production of pion in S waves is naturally expected to be dominant. When going beyond threshold, other partial waves contribute to the production

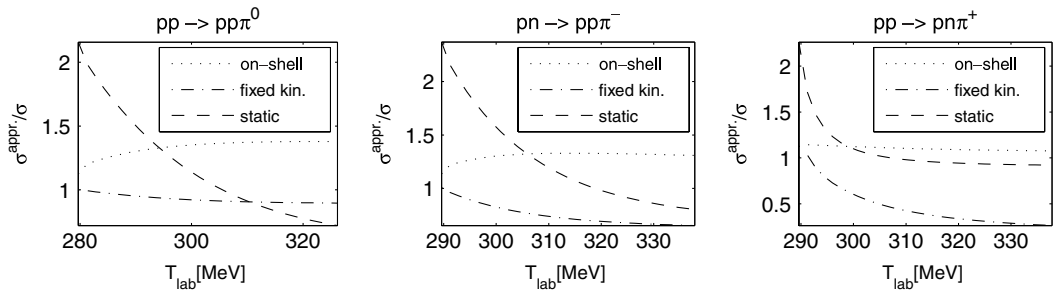

FIG. 2. Ratio between the cross section calculated with different approximations and the S-matrix cross section.

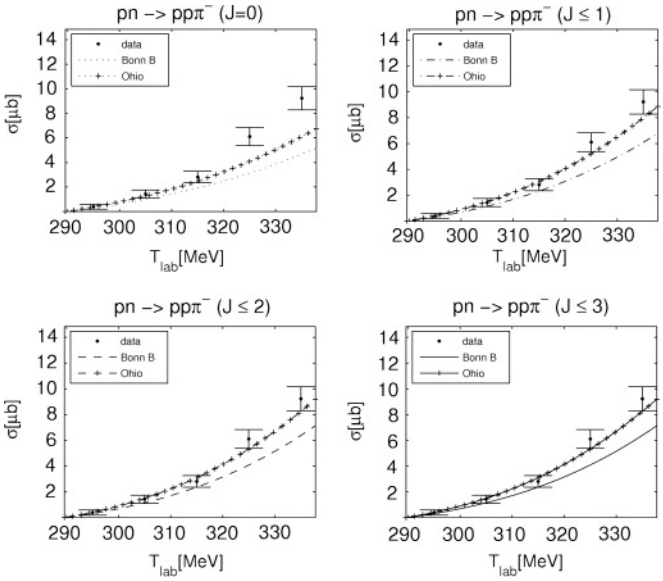

FIG. 4. Same as Fig. 3, but for the $pn \to pp\pi^-$ cross section. Data points are from Ref. [22].

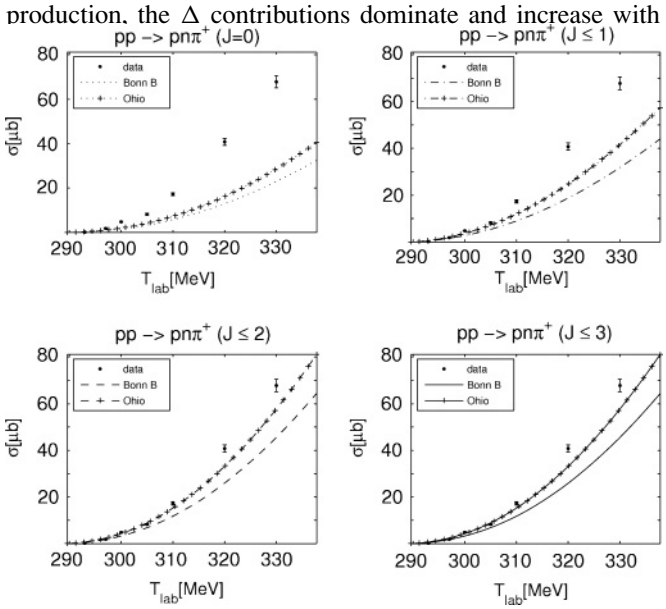

FIG. 5. Same as Fig. 3, but for the $pp \to pn\pi^+$ cross section. Data points are from Ref. [23].

cross section, and as expected, the importance of channels with high J increases with increasing laboratory energy $T_{\rm lab}$. For π^0 production, the $J = 0$ channels alone describe the data and suffice for convergence (Fig. 3). However, for π^- production (Fig. 4) the $J = 1$ channels are needed in addition. For π^+ production (Fig. 5), the convergence is slower than in the other two reactions, as the $J = 2$ channels are necessary for convergence, reflecting the importance of the ${}^1D_2$ NN channel, given its coupling to the ${}^5S_2$ $N\Delta$ channel. It is clear from Figs. 4 and 5 that the description of the charged-pion reactions results from the inclusion of partial waves with high J and that for the π^+ production case (last panel of Fig. 2), the energy dependence of the effective operators is important.

The relative weight of the considered production mechanisms is discussed in detail in Ref. [19]. As in other similar models, the direct production and rescattering mechanisms alone are not sufficient to describe the π^0 production data. In our calculations, the data for π^0 production are described by including the Z diagrams with σ and ω exchanges, which yield about 95% of the cross section for a projectile laboratory energy of 320 MeV. For π^- and π^+ production at the same energy, they contribute about 73% and 36%, respectively. For π^+ production, the Weinberg-Tomozawa term, which does not contribute to π^0 production, is relatively important. The cross sections obtained do not depend crucially on the NN interaction models. We want to point out that the energy dependence of the ${}^1S_0$ NN phase shift beyond 250 MeV is better described by the Ohio NN model, which may cause the differences in the production cross sections for the charged pions, already visible when only $J = 0$ contributions are considered. For π^+ production, the Δ contributions dominate and increase with energy. Some of the general trends obtained here were also found for the Jülich model [24]. In Ref. [24], the short-range mechanisms are included through ω exchange and adjusted to reproduce the total $pp \to pp\pi^0$ cross section close to threshold. In our calculation, no such adjustment is made.

To conclude, by applying the S-matrix approach to the energy-dependent production operators, we achieved an overall description of the cross sections near threshold for charged- and neutral-pion production. Certainly, the model is not complete, e.g., the Coulomb interaction is omitted, and some of the so-called p-wave operators discussed in Ref. [25] and considered in [26] are not included. The production operator via the Δ isobar does not include ρ exchange, which may reduce its contribution, and will be investigated in the future. Nevertheless, our results quantify (i) the sensitivity to the energy dependence of the effective operators, especially for the π^+ reaction, (ii) the importance of higher partial waves in the charged-pion production reactions, and (iii) the dependence on the NN interaction, valid also above the pion production threshold. These findings should survive in even more complete calculations of the production operator and may be tested on the polarization observables.

V.M. was supported by Grant No. SFRD/BD/4876/2001, M.T.P. by Grant No. POCTI/FNU/50358/2002, and J.A. by the Grant Nos. GA CR 202/03/0210 and GA CR 202/06/0746. Ch.E. acknowledges the support of the U.S. Department of Energy under Contract No. DE-FG02-93ER40756 with Ohio University.

[1] H. Machner and J. Haidenbauer, J. Phys. G **25**, R231 (1999); C. Hanhart, Phys. Rep. **397**, 155 (2004).

[2] A. Gardestig, D. R. Phillips, and C. Elster, Phys. Rev. C **73**, 024002 (2006); V. Lensky, V. Baru, J. Haidenbauer, C. Hanhart, A. E. Kudryavtsev, and U. G. Meissner, Eur. Phys. J. A **27**, 37 (2006).

[3] C. Hanhart and N. Kaiser, Phys. Rev. C **66**, 054005 (2002).

[4] J. A. Niskanen, Phys. Lett. **B642**, 34 (2006).
[5] T. S. H. Lee and D. O. Riska, Phys. Rev. Lett. **70**, 2237 (1993); M. T. Peña, D. O. Riska, and A. Stadler, Phys. Rev. C **60**, 045201 (1999).
[6] J. A. Niskanen, Phys. Rev. C **53**, 526 (1996).
[7] T. D. Cohen, J. L. Friar, G. A. Miller, and U. van Kolck, Phys. Rev. C **53**, 2661 (1996).
[8] B. Y. Park, F. Myhrer, J. R. Morones, T. Meissner, and K. Kubodera, Phys. Rev. C **53**, 1519 (1996).
[9] C. Hanhart, J. Haidenbauer, M. Hoffmann, U. G. Meissner, and J. Speth, Phys. Lett. **B424**, 8 (1998).
[10] C. A. da Rocha, G. A. Miller, and U. van Kolck, Phys. Rev. C **61**, 034613 (2000).
[11] C. Hanhart, G. A. Miller, F. Myhrer, T. Sato, and U. van Kolck, Phys. Rev. C **63**, 044002 (2001); A. Motzke, C. Elster, and C. Hanhart, *ibid.* **66**, 054002 (2002).
[12] T. Sato, T. S. H. Lee, F. Myhrer, and K. Kubodera, Phys. Rev. C **56**, 1246 (1997).
[13] V. Malafaia, J. Adam, Jr., and M. T. Peña, Phys. Rev. C **71**, 034002 (2005).
[14] V. Malafaia and M. T. Peña, Phys. Rev. C **69**, 024001 (2004).
[15] V. Bernard, N. Kaiser, and U. G. Meissner, Nucl. Phys. **A615**, 483 (1997).
[16] E. Epelbaum, Prog. Part. Nucl. Phys. **57**, 654 (2006).
[17] Ch. Elster, K. Holinde, D. Schutte, and R. Machleidt, Phys. Rev. C **38**, 1828 (1988); A. Schwick, Ch. Elster, A. Gardestig, and F. Hinterberger (EDDA Collaboration), in preparation; A. Schwick, Diploma thesis, U. Bonn (2004).
[18] SAID program, Center for Nuclear Studies and Data Analysis Center, George Washington University, http://gwdac.phys.gwu.edu.
[19] V. Malafaia, M. T. Peña, Ch. Elster, and J. Adam, in preparation; V. Malafaia, Ph.D. thesis, IST Lisbon (2005), nucl-th/0602026.
[20] R. Machleidt, Adv. Nucl. Phys. **19**, 189 (1989).
[21] H. O. Meyer *et al*., Nucl. Phys. **A539**, 633 (1992).
[22] M. G. Bachman *et al*., Phys. Rev. C **52**, 495 (1995).
[23] J. G. Hardie *et al*., Phys. Rev. C **56**, 20 (1997).
[24] C. Hanhart, J. Haidenbauer, A. Reuber, C. Schutz, and J. Speth, Phys. Lett. **B358**, 21 (1995); C. Hanhart, J. Haidenbauer, O. Krehl, and J. Speth, Phys. Lett. **B444**, 25 (1998).
[25] C. Hanhart, U. van Kolck, and G. A. Miller, Phys. Rev. Lett. **85**, 2905 (2000).
[26] V. Bernard, N. Kaiser, and U. G. Meissner, Eur. Phys. J. A **4**, 259 (1999).